

Onset of spatiotemporal intermittency in a coupled-map lattice

John R. de Bruyn and Lihong Pan

Department of Physics, Memorial University of Newfoundland, St. John's, Newfoundland, Canada A1B 3X7

(Received 14 December 1992)

We have investigated numerically the onset of spatiotemporal intermittency in a one-dimensional lattice of coupled nonlinear maps. The phase boundary between the laminar and intermittent states has a complicated form, with several reentrant regions. Using finite-size scaling, we have determined the critical exponents associated with the transition to spatiotemporal intermittency for several values of the map's coupling parameter. The exponents appear to be nonuniversal in the weak-coupling limit of the map.

PACS number(s): 05.45.+b

While the study of chaotic behavior in spatially confined systems is well developed [1], our understanding of chaos in systems with many spatial degrees of freedom is much less advanced. Experiments on Rayleigh-Bénard convection [2,3] and the printer's instability [4] have demonstrated that chaos in extended quasi-one-dimensional systems can take the form of spatiotemporal intermittency (STI). In this state, slowly evolving regions of ordered ("laminar") and disordered ("turbulent") appearance coexist. Both the spatial extent and the temporal lifetime of these regions fluctuate. Similar behavior has been studied in systems of coupled partial-differential equations [5], nonlinear maps [6–10], and cellular automata [8], and STI seems to be an important step on the route to full turbulence in extended one-dimensional systems.

Coupled-map lattices (CML's) are arrays of lattice points, each of which has a local dynamics governed by an iterative (nonlinear) map. Coupling of a lattice point's dynamics to that of its neighbors models the coupling of spatial degrees of freedom in an extended system. In CML's, both space and time are discretized, but the range of values that can be assigned to a site is continuous. CML's can thus be viewed as models of reality intermediate between fully continuous partial-differential equations and fully discretized cellular automata.

The transition from completely laminar behavior to STI in CML's has been studied by several groups [7,10]. The transition displays features analogous to those seen in equilibrium critical phenomena—for example, spatial correlation lengths and relaxation times that diverge as the transition is approached, and the equivalent of an order parameter that goes to zero at the transition. In CML's, however, as in laboratory dynamical systems, the transition to STI is a nonequilibrium process. Houlrik, Webman, and Jensen [10] have applied ideas and techniques from the study of equilibrium phase transitions to the transition in a CML, and studied the way in which the system behavior scales with lattice size in the critical region. They have calculated, numerically and in two mean-field approximations, the phase diagram for this transition. From their numerical results and a finite-size scaling analysis, they extract critical exponents for the

transition to STI for a few values of the system parameters.

In this paper we present the results of some numerical calculations of the transition to STI in the coupled-map system earlier studied by Houlrik, Webman, and Jensen [10]. Our initial goal was to investigate a suggestion made by them that the critical exponents characterizing this transition may be universal over some range of the map's parameter space. The calculation of critical exponents over the entire parameter range with an accuracy sufficient to permit a meaningful discussion of their universality, or the absence thereof, would, however, have required time and computing resources unavailable to us. We content ourselves, therefore, with presenting a more detailed picture of the phase boundary between laminar and STI states, and values of the critical exponents for several more values of the system parameters, mostly in the weak-coupling limit of the map.

The one-dimensional coupled-map lattice we studied is the map used by Houlrik, Webman, and Jensen [10] and Chaté and Manneville [7], and is defined by

$$x_i^n = (1 - \epsilon)x_i^{n-1} + \frac{\epsilon}{2}[f(x_{i-1}^{n-1}) + f(x_{i+1}^{n-1})]. \quad (1)$$

Here ϵ is the strength of a diffusive coupling between nearest-neighbor sites on the lattice. The subscript is a site index and the superscript the iteration number. The local mapping $f(x)$ is a modified tent map given by

$$f(x) = \begin{cases} rx & (0 \leq x \leq \frac{1}{2}) \\ r(1-x) & (\frac{1}{2} \leq x \leq 1) \\ x & (1 < x \leq r/2). \end{cases} \quad (2)$$

The parameter $r > 2$ can be viewed as a control parameter or "temperature" variable. This local map displays transient chaos [11]; that is, sites iterate chaotically until they eventually escape to the line of stable fixed points $1 < x \leq r/2$. For larger r , the "escape window" is larger and the length of the transient is correspondingly smaller. Following established terminology, we refer to chaotic sites as turbulent and nonchaotic sites as laminar. The nearest-neighbor coupling in Eq. (1) allows laminar sites

to be pulled back into the turbulent state by their neighbors, and leads to the development of STI.

As discussed by Houlrik, Webman, and Jensen [10], the way in which the critical behavior of the CML on finite lattices scales with lattice size L can be analyzed to give the true, infinite-lattice critical behavior. Since we make use of the results of their calculations, we summarize them here. We define the “order parameter” m to be the mean number of turbulent sites on the lattice, i.e., those sites for which $x_i \leq 1$. Since the finite system does not evolve to a well-defined steady state, m is time dependent, and eventually goes to zero in a characteristic absorption time τ . At fixed r , the transition to STI occurs at a critical value of $\epsilon = \epsilon_c(r)$. When ϵ is on the laminar side of ϵ_c , τ grows logarithmically with L , while for ϵ on the chaotic side of ϵ_c , τ grows exponentially. At criticality,

$$\tau \sim L^z, \quad (3)$$

where $z = \nu_{\parallel}/\nu_{\perp}$ is a dynamical critical exponent. ν_{\parallel} is the critical exponent characterizing the divergence of the absorption time as $|\epsilon - \epsilon_c| \rightarrow 0$:

$$\tau \sim |\epsilon - \epsilon_c|^{-\nu_{\parallel}}, \quad (4)$$

and ν_{\perp} is the analogous exponent for the correlation length, i.e., the characteristic size of the laminar regions. For small times ($t \ll L^z$), m behaves like

$$m \sim t^{-\beta/\nu_{\parallel}}, \quad (5)$$

while for long times ($t \gg L^z$),

$$m \sim e^{-t/L^z}. \quad (6)$$

The critical exponent β characterizes the order parameter’s approach to zero as $\epsilon \rightarrow \epsilon_c$ from within the STI phase. Using these relations, we can determine the exponents β , ν_{\parallel} , and ν_{\perp} from the results of our numerical calculations, as was done by Houlrik, Webman, and Jensen in Ref. [10] and illustrated in their Figs. 8 and 9.

Our calculations were done on one-dimensional lattices of size $L = 2^n$, for $3 \leq n \leq 11$, with periodic boundary conditions. The site values x_i were initialized to random values between 0 and 1 and the map iterated until m evolved to zero. Typically 300 to 1000 runs were averaged for analysis. Initial estimates of $\epsilon_c(r)$, accurate to

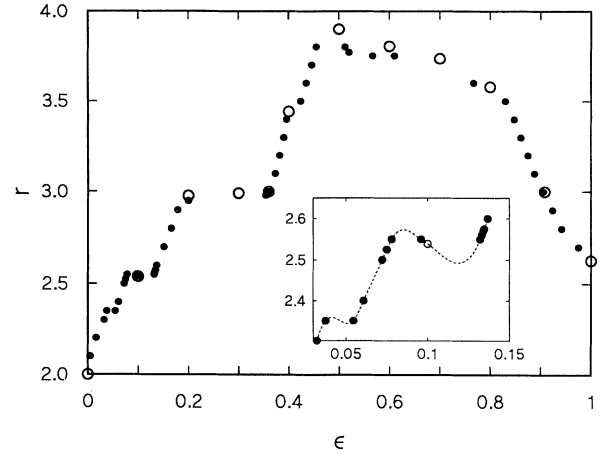


FIG. 1. The phase diagram of the coupled-map lattice. The system is laminar above the plotted data and spatiotemporally intermittent below. ●, points calculated in the present work; ○, points taken from Ref. [10]. The inset shows the low- ϵ region in more detail; the curve through the points is a guide to the eye only and greatly exaggerates the range in r of the loops in the phase boundary.

plus or minus a few times 10^{-3} , were obtained by inspection of plots of $\log \tau$ against $\log L$, for $L \leq 512$, bearing in mind Eq. (3). Critical exponents were evaluated from calculations on lattices with $L \leq 2048$ and correspondingly more refined values of ϵ_c , making use of the scaling relationships given in Eqs. (3)–(5).

Figure 1 shows the calculated phase diagram for this system. The system is ordered above the plotted data and in the STI state below. We also show in Fig. 1 the points calculated by Houlrik, Webman, and Jensen [10]. The phase boundary has a rather complicated form. The phase diagram is reentrant over most of the range of r , in the sense that, for fixed r , increasing ϵ takes the system from the laminar phase to STI and back to the laminar phase again. There are also several ranges of r for which the model has multiply reentrant behavior. The inset to Fig. 1 shows the small- ϵ region of the phase diagram on an expanded scale. There are three values of ϵ_c shown for $r = 2.35$, in the range $0.040 \lesssim \epsilon \lesssim 0.046$, and similarly for $r = 2.55$ in the range $0.085 \lesssim \epsilon \lesssim 0.135$. These reentrant regions each span a very small range of r ;

TABLE I. Numerically determined values of the critical exponents and exponent ratios.

r	ϵ_c	z	β/ν_{\parallel}	β	ν_{\parallel}	ν_{\perp}
2.2	0.016 08(2)	1.684(6)	0.146(6)	0.26(3)	1.8(1)	1.1(1)
2.3	0.032 18(2)	1.44(2)	0.198(6)	0.32(1)	1.66(2)	1.15(3)
2.4	0.060 90(2)	1.39(2)	0.252(6)	0.36(1)	1.42(2)	1.02(3)
2.5	0.072 28(6)	1.51(2)	0.243(6)	0.31(1)	1.26(2)	0.83(2)
2.539	0.100 0(1)	1.43(2)				
2.6	0.136 72(4)	1.25(2)	0.189(6)	0.28(1)	1.48(2)	1.18(4)
2.7	0.151 15(5)	1.43(2)	0.186(6)	0.26(1)	1.41(2)	0.99(3)
3.4	0.395 50(25)	1.19(3)	0.27(2)			
3.7	0.446 0(5)	1.12(2)	0.33(2)	0.24(1)	0.75(2)	0.67(2)
3.4	0.847 5(3)	1.64(2)	0.14(1)	0.20(1)	1.47(4)	0.90(3)
3.77	0.520 0(5)	1.24(2)	0.33(2)	0.27(2)	0.83(3)	0.66(3)

the curve through the points in the inset to Fig. 1 is a guide to the eye only and greatly exaggerates the size of the “loops.” We have numerically found a similar region near $r=3.75$, $\epsilon=0.6$. From the appearance of the phase boundary, there is most likely another of these regions between $\epsilon \approx 0.2$ and $\epsilon \approx 0.36$ near $r=3$, and possibly others elsewhere, although we have not confirmed this.

Figures 2(a)–2(e) show the exponent ratios z and β/ν_{\parallel} ,

and the critical exponents β , ν_{\parallel} , and ν_{\perp} plotted as a function of ϵ_c ; these quantities are also tabulated in Table I. We determined ϵ_c to an accuracy of on the order of $\pm 10^{-4}$ or better from log-log plots of τ vs L , for different values of ϵ . ϵ_c was taken as that value for which τ most nearly grew as a power law in lattice size. The exponent z was obtained from fits of $\tau(L)$ to Eq. (3). The errors given include a contribution to account for the uncertain-

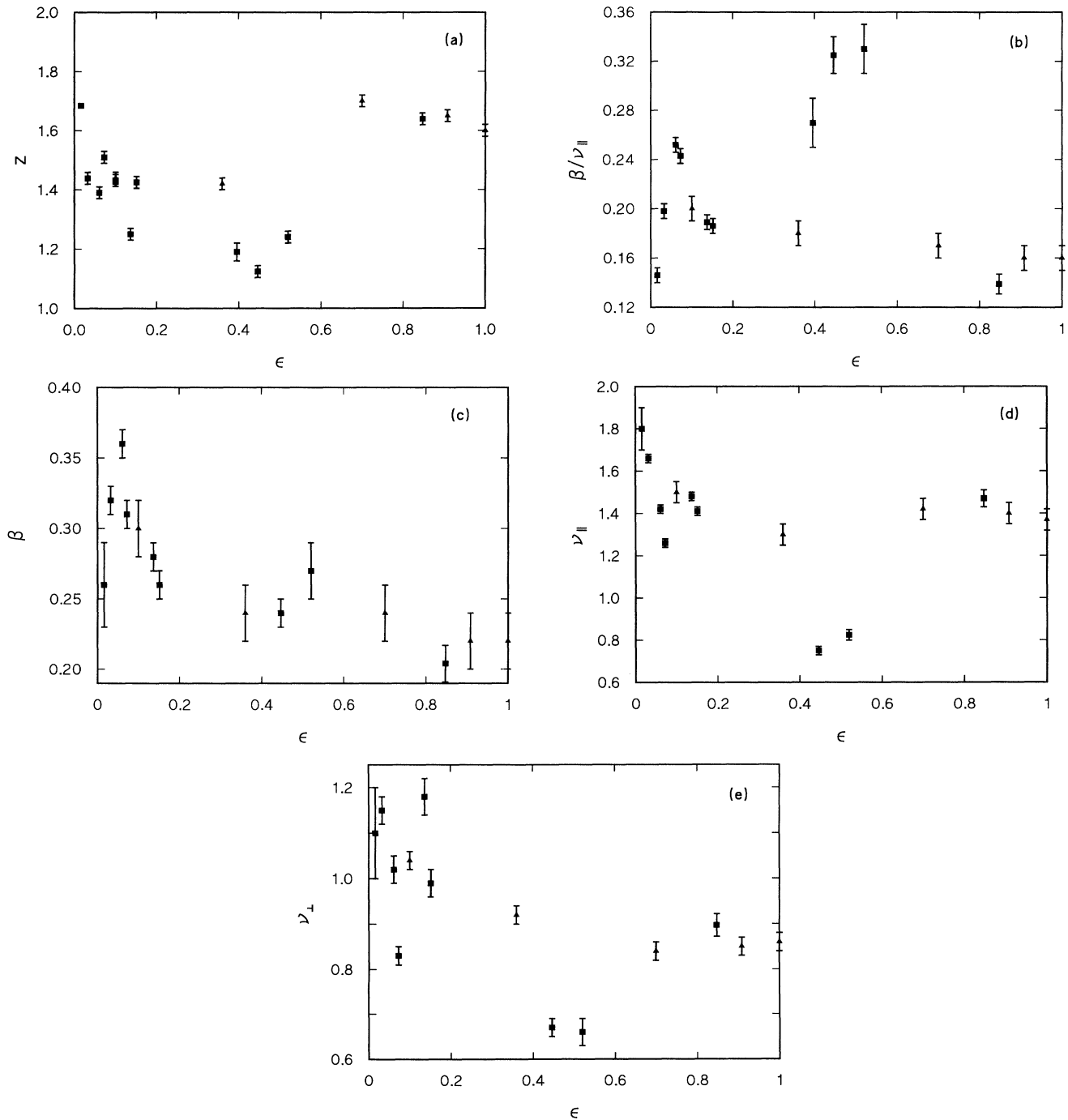


FIG. 2. The critical exponents and exponent ratios for the onset of spatiotemporal intermittency, plotted as a function of the critical value of the control parameter ϵ . (a) $z = \nu_{\parallel}/\nu_{\perp}$; (b) β/ν_{\parallel} ; (c) β ; (d) ν_{\parallel} ; (e) ν_{\perp} . ■, present work; ▲, results of Ref. [10].

ty in ϵ_c . The ratio β/ν_{\parallel} was determined from the slopes of log-log plots of m vs t (where the time t is given by the iteration number) calculated at $\epsilon = \epsilon_c$, at times short compared to L^z , but neglecting initial-condition-dependent behavior observed over the first few iterations. ν_{\parallel} was obtained from log-log plots of τ vs $|\epsilon - \epsilon_c|$. From these quantities the exponents β and ν_{\parallel} were calculated.

From the graphs shown in Fig. 2 it can be seen that, at low values of ϵ , i.e., in the weak-coupling limit of the map, all of the critical exponents and exponent ratios vary nonsystematically by substantially more than the size of the error bars, and appear to depend in a complicated way on the coupling parameter. The exponents thus appear to be nonuniversal in the weak-coupling limit, although of course we cannot make any statement about the values of the exponents between the points which we calculated.

We have added only one point to the results of Ref. [10] for values of $\epsilon \gtrsim 0.7$, but the exponents for our new point agree within error with the previous results. Cer-

tainly there is much less variation in the exponent values in this range than at low ϵ , and it remains possible that the transition to spatiotemporal intermittency in the strong-coupling limit is described by a small number of universality classes.

We have numerically calculated the boundary between the laminar and spatiotemporally intermittent states of a nonlinear coupled-map lattice, and determined the associated critical exponents for a few values of the system parameters. We have demonstrated that the phase boundary has a rather complicated, multiply reentrant form. The critical exponents appear to be nonuniversal in the weak-coupling limit of the map, but at stronger values of the coupling parameter universality remains a possibility; further work is required to resolve this issue.

This research was supported by the Natural Sciences and Engineering Research Council of Canada. We are grateful to J. Whitehead and M. Whitmore for allowing us the extensive use of their computing facilities.

-
- [1] S. N. Rasband, *Chaotic Dynamics of Nonlinear Systems* (Wiley, New York, 1990).
 - [2] S. Ciliberto and P. Bigazzi, *Phys. Rev. Lett.* **60**, 286 (1988).
 - [3] F. Daviaud, M. Dubois, and P. Bergé, *Europhys. Lett.* **9**, 441 (1989); F. Daviaud, M. Bonnetti, and M. Dubois, *Phys. Rev. A* **42**, 3388 (1990).
 - [4] M. Rabaud, S. Michalland, and Y. Couder, *Phys. Rev. Lett.* **64**, 184 (1990).
 - [5] H. Chaté and P. Manneville, *Phys. Rev. Lett.* **58**, 112 (1987).
 - [6] K. Kaneko, *Prog. Theor. Phys.* **74**, 1033 (1985).
 - [7] H. Chaté and P. Manneville, *Physica D* **32**, 409 (1988).
 - [8] H. Chaté and P. Manneville, *J. Stat. Phys.* **56**, 357 (1989).
 - [9] H. Sakaguchi, *Prog. Theor. Phys.* **80**, 7 (1988).
 - [10] J. M. Houlrik, I. Webman, and M. H. Jensen, *Phys. Rev. A* **41**, 4210 (1990).
 - [11] C. Grebogi, E. Ott, and J. A. Yorke, *Phys. Rev. Lett.* **57**, 1284 (1986).